Frontiers of Information Technology & Electronic Engineering
www.zju.edu.cn/jzus; engineering.cae.cn; www.springerlink.com
ISSN 2095-9184 (print); ISSN 2095-9230 (online)
E-mail: jzus@zju.edu.cn

Joint DOA and channel estimation with data detection based on 2D unitary ESPRIT in massive MIMO systems*

Jing-ming KUANG, Yuan ZHOU, Ze-song FEI‡

(*School of Information and Electronics, Beijing Institute of Technology, Beijing 100081, China*)

E-mail: jmkuang@bit.edu.cn; zhouyuanbit@163.com; feizesong@bit.edu.cn

Received Jan. 9, 2017; Revision accepted Apr. 20, 2017; Crosschecked June 9, 2017

Abstract: We propose a novel method for joint two-dimensional (2D) direction-of-arrival (DOA) and channel estimation with data detection for uniform rectangular arrays (URAs) for the massive multiple-input multiple-output (MIMO) systems. The conventional DOA estimation algorithms usually assume that the channel impulse responses are known exactly. However, the large number of antennas in a massive MIMO system can lead to a challenge in estimating accurate corresponding channel impulse responses. In contrast, a joint DOA and channel estimation scheme is proposed, which first estimates the channel impulse responses for the links between the transmitters and antenna elements using training sequences. After that, the DOAs of the waves are estimated based on a unitary ESPRIT algorithm using previous channel impulse response estimates instead of accurate channel impulse responses and then, the enhanced channel impulse response estimates can be obtained. The proposed estimator enjoys closed-form expressions, and thus it bypasses the search and pairing processes. In addition, a low-complexity approach toward data detection is presented by reducing the dimension of the inversion matrix in massive MIMO systems. Different cases for the proposed method are analyzed by changing the number of antennas. Experimental results demonstrate the validity of the proposed method.

Key words: Two-dimensional (2D) direction-of-arrival (DOA) estimation; Channel impulse response estimation; Data detection; Uniform rectangular array (URA); Massive multiple-input multiple-output (MIMO)

http://dx.doi.org/10.1631/FITEE.1700025 **CLC number:** TN828.6

1 Introduction

The massive multiple-input multiple-output (massive MIMO) technique, a key technology of fifth generation (5G) wireless systems (Marzetta, 2010; Rusek *et al.*, 2013), has attracted increasing attention due to its improved throughput, spectral efficiency, and link reliability (Larsson *et al.*, 2014). In a massive MIMO system, each base station (BS) is equipped with a large number of antennas with the objective of serving a number of single-antenna mobile stations (MSs) that simultaneously occupy the same set of time and frequency resources (Lan *et al.*, 2016). It is well known that the beamforming performance in massive MIMO systems relies closely on the accuracy of the estimated direction-of-arrival (DOA) (Hu *et al.*, 2014). The antenna arrays of massive MIMO systems are meant to be implemented in more than one dimension because of the constraints concerning array aperture. The extension of the antenna array dimension offers flexibility at the terminal, specifically for spatial pre-processing in both horizontal and vertical domains. Consequently, estimating the azimuth and elevation angles efficiently and accurately is a crucial problem.

DOA estimation has been of interest for decades across a broad range of signal processing technologies including radar, sonar, and wireless communications. There are many existing methods, such as maximum likelihood (ML) spectral estimation (Capon, 1983),

‡ Corresponding author

* Project supported by Ericsson and the National Natural Science Foundation of China (No. 61371075)

ORCID: Ze-song FEI, http://orcid.org/0000-0002-7576-625X

multiple signal classification (MUSIC) (Schmidt, 1986), Root-MUSIC (Barabell, 1983), estimation of signal parameters via rotational invariance techniques (ESPRIT) (Roy and Kailath, 1989), and unitary ESPRIT (Haardt and Nossek, 1995), to estimate the one-dimensional (1D) and two-dimensional (2D) DOAs. Recently, 2D DOA estimation algorithms for massive MIMO systems were studied. In Yang *et al.* (2014), a two-stage low-complexity DOA estimation scheme was proposed by performing two MUSIC algorithms for estimating, respectively, the azimuth and elevation angles of the impinging sources. The algorithm requires a multi-dimensional spectrum peak search, resulting in a relatively high computational complexity as in most 2D DOA estimation algorithms. The ESPRIT based 2D DOA estimation without spectrum peak search was characterized in Zhu *et al.* (2013) and Liu *et al.* (2014), where a pairing process for the azimuth and elevation angles was needed. To further abandon the pairing process, unitary ESPRIT based 2D DOA estimation was used in Wang *et al.* (2012) and Wang *et al.* (2015). Pioneering works considered the DOA estimation under a limitation that the channel impulse responses are known.

Because of the huge number of sensors, it is very challenging for a base station to estimate the accurate corresponding channel impulse responses before DOA estimation. D'Amico *et al.* (2004) and D'Amico and Morelli (2009) studied the problem of joint channel and DOA estimation, and considered a CDMA network in which the base station is endowed with a uniform linear array (ULA). D'Amico(2004) proposed an approach based on training symbols and a 1D search, and D'Amico and Morelli (2009) followed an ML approach. These approaches proposed in D'Amico *et al.* (2004) and D'Amico and Morelli (2009) need a search process, which is not suitable for massive MIMO systems. Zhang *et al.* (2015) used the rotational invariance of array channel impulse responses and estimated the DOA of arriving paths individually for a ULA. Alibi *et al.* (2016) described a novel method for 2D DOA estimation for a uniform circular array (UCA) using channel state information (CSI); however, the method needs a spectrum peak search process. To the best of the authors' knowledge, no study has so far dealt with the problem of joint DOA and channel estimation for a uniform rectangular array (URA) in a massive MIMO system. To handle the problem of DOA estimation and channel estimation, the development of low-complexity joint DOA and channel estimation algorithms for massive MIMO systems has become imperative from the perspective of practical implementation.

In this paper, we propose a joint estimator of DOA and channel impulse responses with data detection based on a URA in a massive MIMO system. The channel impulse responses for the links between the transmitters and each of the array elements are estimated in the first step. In the second step, 2D DOA estimation can be obtained using a 2D unitary ESPRIT algorithm based on estimated channel impulse responses with estimation errors. The azimuth- and elevation-angle estimations do not need spectrum peak search or additional pairing operations. After that, the DOAs of the impinging wavefronts can be exploited to estimate the channels associated with different DOAs. Thus, this novel approach provides an enhanced channel estimation by improving the channel impulse response estimation determined in the first step. In this way, the directional inhomogeneity of the mobile radio channel is exploited, since the actual channel impulse responses are estimated but not the links between every user and each array element. Furthermore, the orthogonality of the steering vectors in the massive MIMO system for a URA is derived with the azimuth and elevation angles of arrival drawn independently from a continuous distribution. In addition, a low-complexity data detection scheme will be presented by transforming an inverse of a $KD \times KD$ matrix to K inversions of $D \times D$ matrices, based on the above-mentioned enhanced channel impulse response estimates and their DOAs.

Throughout our discussion, $\mathbb{C}$ denotes the complex number field. Lower- and upper-case boldface symbols denote vectors and matrices, respectively, while underlined boldface upper-case symbols denote column vectors. $\boldsymbol{I}_K$ denotes the $K \times K$ identity matrix and $\mathbf{0}$ is the zero vector with an appropriate dimension, while $[\cdot]_i$ is the ith element of a vector. The symbol $\otimes$ denotes a Kronecker product. Operations $(\cdot)^{\mathrm{T}}$, $(\cdot)^*$, $(\cdot)^{\mathrm{H}}$, and $(\cdot)^\dagger$ denote transpose, conjugate, conjugate transpose, and pseudoinverse, respectively. $\mathrm{diag}(a_1, a_2, \cdots, a_M)$ is the diagonal matrix with $a_1, a_2, \cdots, a_M$ as its diagonal elements, while j denotes the imaginary axis. $\mathrm{vec}\{\boldsymbol{X}\}$ defines the column stacking operator which stacks

the columns of $\boldsymbol{X}$ into a vector, while $\boldsymbol{\Pi}_M$ is the $M \times M$ exchange matrix with ones on its anti-diagonal elements and zeros elsewhere.

2 System model

Assume the far-field narrow-band echoes of K incoherent sources impinging on the URA locate in the (x, y) plane (Fig. 1). The URA is composed of M antenna elements in the x-direction and N antenna elements in the y-direction with an array element spacing d. The number of resolvable multipaths of the kth user is P_k. The azimuth and elevation angles for the pth path of a signal coming from transmitter k are denoted by φ_p^k and θ_p^k, respectively.

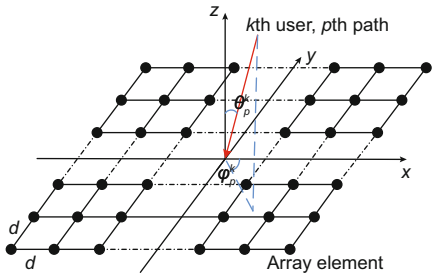

Fig. 1 System model

Let $\boldsymbol{X}_k$ $(k = 1, 2, \ldots, K)$ denote the $L \times W$ Toeplitz matrix of the training sequence for the kth user. Here, L is the number of samples of the received signal depending exclusively on the training sequence but not on the transmitted data, and W is the channel length. The matrix $\boldsymbol{X}$ of the user specific training sequences, known at the receiver, which will be used for the joint channel estimation, is given by $\boldsymbol{X} = [\boldsymbol{X}_1, \boldsymbol{X}_2, \ldots, \boldsymbol{X}_K] \in \mathbb{C}^{L \times KW}$. The channel impulse responses corresponding to the links between the specific user and each array element are called the combined channel impulse responses, and are not connected with DOAs. The combined channel impulse responses from the kth user can be expressed as

$$\boldsymbol{G}_k = [\boldsymbol{g}_1^k, \boldsymbol{g}_2^k, ..., \boldsymbol{g}_{MN}^k], \tag{1}$$

where the discrete time channel impulse responses $\boldsymbol{g}_i^k$ of length W can be obtained by

$$\boldsymbol{g}_i^k = \sum_{p=1}^{P_k} \boldsymbol{h}_p^k [\boldsymbol{a}_p^k]_i, \tag{2}$$

$i = (m-1)N + n$, $n = 1, 2, \ldots, N$, $m = 1, 2, \ldots, M$, $\boldsymbol{h}_p^k = [h_{p1}^k, h_{p2}^k, \ldots, h_{pW}^K]^{\mathrm{T}} \in \mathbb{C}^{W \times 1}$ are the channel impulse responses for the pth path of the kth user and have length W, and $\boldsymbol{a}_p^k \in \mathbb{C}^{MN \times 1}$ is the steering vector for the pth path of the kth user:

$$[\boldsymbol{a}_p^k]_i = \exp\left\{ \mathrm{j} \left[\left(m - \frac{M+1}{2} \right) u_p^k + \left(n - \frac{N+1}{2} \right) v_p^k \right] \right\}, \tag{3}$$

where

$$\begin{cases} u_p^k = 2\pi \dfrac{d}{\lambda} \cos\varphi_p^k \sin\theta_p^k, \\ v_p^k = 2\pi \dfrac{d}{\lambda} \sin\varphi_p^k \sin\theta_p^k, \end{cases}$$

and λ is the carrier frequency. We refer to $\boldsymbol{h}_p^k$ as the directional channel impulse responses, which means that the channels depend on the DOA of each user (Blanz *et al.*, 2000), to distinguish them from the combined channel impulse responses $\boldsymbol{g}_i^k$ connected with the array elements. We arrange the combined channel impulse responses from all users to a matrix $\boldsymbol{G} = [\boldsymbol{G}_1^{\mathrm{T}}, \boldsymbol{G}_2^{\mathrm{T}}, \ldots, \boldsymbol{G}_K^{\mathrm{T}}]^{\mathrm{T}} \in \mathbb{C}^{KW \times MN}$.

The directional channel impulse responses for the kth user is a $W \times P_k$ matrix denoted as follows:

$$\boldsymbol{H}_k = [\boldsymbol{h}_1^k, \boldsymbol{h}_2^k, \ldots, \boldsymbol{h}_{P_k}^k], k = 1, 2, \ldots, K, \tag{4}$$

and the $MN \times P_k$ steering matrix for the kth user is combined as

$$\boldsymbol{A}_k = [\boldsymbol{a}_1^k, \boldsymbol{a}_2^k, \ldots, \boldsymbol{a}_{P_k}^k], k = 1, 2, \ldots, K. \tag{5}$$

With steering matrix $\boldsymbol{A}_k$ and directional channel impulse responses $\boldsymbol{H}_k$, the relationship between the combined channel impulse responses for the kth user contained in matrix $\boldsymbol{G}_k$ and directional channel impulse responses for the kth user contained in matrix $\boldsymbol{H}_k$ is given by

$$\boldsymbol{G}_k = \sum_{p=1}^{P_k} \boldsymbol{h}_p^k (\boldsymbol{a}_p^k)^{\mathrm{T}} = \boldsymbol{H}_k \boldsymbol{A}_k^{\mathrm{T}}. \tag{6}$$

Then, the received signals $\boldsymbol{Y}$ at the URA from all K users are given by

$$\begin{aligned} \boldsymbol{Y} &= \boldsymbol{X}\boldsymbol{G} + \boldsymbol{Z} \\ &= [\boldsymbol{X}_1, \boldsymbol{X}_2, \ldots, \boldsymbol{X}_K] \\ &\quad \cdot [\boldsymbol{A}_1 \boldsymbol{H}_1^{\mathrm{T}}, \boldsymbol{A}_2 \boldsymbol{H}_2^{\mathrm{T}}, \ldots, \boldsymbol{A}_K \boldsymbol{H}_K^{\mathrm{T}}]^{\mathrm{T}} + \boldsymbol{Z} \\ &= \sum_{k=1}^{K} \boldsymbol{X}_k \boldsymbol{H}_k \boldsymbol{A}_k^{\mathrm{T}} + \boldsymbol{Z}, \end{aligned} \tag{7}$$

where $\boldsymbol{Z} = [\boldsymbol{Z}_1, \boldsymbol{Z}_2, \ldots, \boldsymbol{Z}_{MN}] \in \mathbb{C}^{L \times MN}$ is the noise matrix for the MN array elements.

3 Joint DOA and channel estimation

In this section, a novel approach to the joint DOA and channel estimation for a URA system is presented. This approach can be divided into three steps, as illustrated individually in this section.

3.1 Combined channel estimation

The least-square (LS) channel estimation method finds the combined channel impulse response estimates $\hat{\boldsymbol{G}}$ by minimizing the cost function $\mathcal{F} = \|\boldsymbol{Y} - \boldsymbol{X}\boldsymbol{G}\|_{\mathrm{F}}^2$, and gives the solution

$$\hat{\boldsymbol{G}} = \boldsymbol{X}^{\dagger}\boldsymbol{Y}. \tag{8}$$

3.2 DOA estimation

According to Eqs. (7) and (8), the estimated combined channel impulse responses matrix $\hat{\boldsymbol{G}}$ can be rewritten as

$$\hat{\boldsymbol{G}} = \boldsymbol{G} + \boldsymbol{X}^{\dagger}\boldsymbol{Z}. \tag{9}$$

The extraction of the blocks $\hat{\boldsymbol{G}}_k^{\mathrm{T}}$ from $\hat{\boldsymbol{G}}^{\mathrm{T}}$ ($k = 1, 2, \ldots, K$) can be described as

$$\hat{\boldsymbol{G}}_k^{\mathrm{T}} = \hat{\boldsymbol{G}}^{\mathrm{T}}(\boldsymbol{u}_k \otimes \boldsymbol{I}_W), \tag{10}$$

where $\boldsymbol{u}_k$ is the $K \times 1$ identity column vector for the kth user, and

$$[\boldsymbol{u}^l]_k = \begin{cases} 1, & l = k, \\ 0, & \text{otherwise}. \end{cases} \tag{11}$$

According to Eq. (10), we can obtain from Eqs. (6) and (9) that

$$\hat{\boldsymbol{G}}_k^{\mathrm{T}} = \boldsymbol{A}_k\boldsymbol{H}_k^{\mathrm{T}} + (\boldsymbol{X}^{\dagger}\boldsymbol{Z})^{\mathrm{T}}(\boldsymbol{u}_k \otimes \boldsymbol{I}_W). \tag{12}$$

Let $\boldsymbol{E}_k = \hat{\boldsymbol{G}}_k^{\mathrm{T}}$, $\boldsymbol{S}_k = \boldsymbol{H}_k^{\mathrm{T}}$, and $\boldsymbol{W}_k = (\boldsymbol{X}^{\dagger}\boldsymbol{Z})^{\mathrm{T}}(\boldsymbol{u}_k \otimes \boldsymbol{I}_W)$. We can obtain the noise corrupted measurement matrix of the kth user composed of W snapshots as follows:

$$\boldsymbol{E}_k = \boldsymbol{A}_k\boldsymbol{S}_k + \boldsymbol{W}_k,\ k = 1, 2, \ldots, K, \tag{13}$$

where $\boldsymbol{S}_k$ and $\boldsymbol{W}_k$ are the signal and noise matrices of the kth user, respectively, and $\boldsymbol{A}_k$ is the array steering matrix that depends on the DOAs of user k. According to Eq. (13), K different DOA estimation processes can be performed. Then we propose a 2D unitary ESPRIT approach with reduced computational burden. The algorithm is used for the estimation of the DOAs for each user.

The 2D steering vector denoted by Eq. (3) can be decomposed to the Kronecker product of two one-dimensional steering vectors in x-direction and y-direction as

$$\boldsymbol{a}_p^k = \boldsymbol{a}_{px}^k \otimes \boldsymbol{a}_{py}^k, \tag{14}$$

where

$$[\boldsymbol{a}_{px}^k]_m = \exp\left\{\mathrm{j}\left(m - \frac{M+1}{2}\right)u_p^k\right\}, m = 1, 2, \ldots, M,$$

and

$$[\boldsymbol{a}_{py}^k]_n = \exp\left\{\mathrm{j}\left(n - \frac{N+1}{2}\right)v_p^k\right\}, n = 1, 2, \ldots, N.$$

Based on the rotational invariance of $\boldsymbol{a}_{px}^k$ and $\boldsymbol{a}_{py}^k$, we can obtain

$$\begin{cases} \mathrm{e}^{\mathrm{j}u_p^k}\boldsymbol{J}_1\boldsymbol{a}_{px}^k = \boldsymbol{J}_2\boldsymbol{a}_{px}^k, \\ \mathrm{e}^{\mathrm{j}v_p^k}\boldsymbol{J}_3\boldsymbol{a}_{py}^k = \boldsymbol{J}_4\boldsymbol{a}_{py}^k, \end{cases} \tag{15}$$

where $\boldsymbol{J}_1 = [\boldsymbol{I}_{M-1}, \boldsymbol{0}]$ and $\boldsymbol{J}_2 = [\boldsymbol{0}, \boldsymbol{I}_{M-1}]$ are the $(M-1) \times M$ selection matrices, and $\boldsymbol{J}_3$ and $\boldsymbol{J}_4$ are defined similar to $\boldsymbol{J}_1$ and $\boldsymbol{J}_2$ with M replaced by N, such that they are $(N-1) \times N$ matrices.

Employing the center of the URA as the phase reference, the array manifold is conjugate centrosymmetric. Then, the unitary matrix defined in Eq. (16) can transform the complex-valued steering vector into a real-valued manifold. If M is odd, the simplest unitary matrix mentioned in Zoltowski *et al.* (1996) is constructed as

$$\boldsymbol{Q}_M = \frac{1}{\sqrt{2}}\begin{bmatrix} \boldsymbol{I}_{(M-1)/2} & \boldsymbol{0} & \mathrm{j}\boldsymbol{I}_{(M-1)/2} \\ \boldsymbol{0} & \sqrt{2} & \boldsymbol{0} \\ \boldsymbol{\Pi}_{(M-1)/2} & \boldsymbol{0} & -\mathrm{j}\boldsymbol{\Pi}_{(M-1)/2} \end{bmatrix}, \tag{16}$$

and if M is even, a unitary matrix is obtained from Eq. (16) by dropping its center row and center column. We can see that $\boldsymbol{Q}_M$ is a sparse unitary matrix that transforms $\boldsymbol{a}_{px}^k$ into an $M \times 1$ real-valued manifold $\boldsymbol{d}_{px}^k = \boldsymbol{Q}_M^{\mathrm{H}}\boldsymbol{a}_{px}^k$. Similarly, we can obtain real-valued manifold $\boldsymbol{d}_{py}^k$. The 2D manifold $\boldsymbol{d}_p^k$ can be obtained by

$$\begin{aligned} \boldsymbol{d}_p^k &= (\boldsymbol{Q}_M^{\mathrm{H}} \otimes \boldsymbol{Q}_N^{\mathrm{H}})\boldsymbol{a}_p^k \\ &= (\boldsymbol{Q}_M^{\mathrm{H}}\boldsymbol{a}_{px}^k) \otimes (\boldsymbol{Q}_N^{\mathrm{H}}\boldsymbol{a}_{py}^k) \\ &= \boldsymbol{d}_{px}^k \otimes \boldsymbol{d}_{py}^k, \end{aligned} \tag{17}$$

where $\boldsymbol{Q}_N$ is defined similar to Eq. (16) with M replaced by N. Take the steering vector in the x-direction $\boldsymbol{a}_{px}^k$ as an example. Based on the fact that

$\boldsymbol{Q}_M$ is unitary, the first equation of Eq. (15) is rewritten as

$$\mathrm{e}^{\mathrm{j}u_p^k}\boldsymbol{J}_1\boldsymbol{Q}_M\boldsymbol{Q}_M^{\mathrm{H}}\boldsymbol{a}_{px}^k=\boldsymbol{J}_2\boldsymbol{Q}_M\boldsymbol{Q}_M^{\mathrm{H}}\boldsymbol{a}_{px}^k. \tag{18}$$

Premultiplying both sides of Eq. (18) by $\boldsymbol{Q}_{M-1}^{\mathrm{H}}$ yields the following invariance relationship:

$$\mathrm{e}^{\mathrm{j}u_p^k}\boldsymbol{Q}_{M-1}^{\mathrm{H}}\boldsymbol{J}_1\boldsymbol{Q}_M\boldsymbol{d}_{px}^k=\boldsymbol{Q}_{M-1}^{\mathrm{H}}\boldsymbol{J}_2\boldsymbol{Q}_M\boldsymbol{d}_{px}^k. \tag{19}$$

Note that $\boldsymbol{Q}_{M-1}^{\mathrm{H}}\boldsymbol{J}_2\boldsymbol{Q}_M=(\boldsymbol{Q}_{M-1}^{\mathrm{H}}\boldsymbol{J}_1\boldsymbol{Q}_M)^*$. Let $\boldsymbol{K}_1$ and $\boldsymbol{K}_2$ be the real and imaginary parts of $\boldsymbol{Q}_{M-1}^{\mathrm{H}}\boldsymbol{J}_2\boldsymbol{Q}_M$, respectively, i.e., $\boldsymbol{K}_1=\mathrm{Re}\{\boldsymbol{Q}_{M-1}^{\mathrm{H}}\boldsymbol{J}_2\boldsymbol{Q}_M\}$ and $\boldsymbol{K}_2=\mathrm{Im}\{\boldsymbol{Q}_{M-1}^{\mathrm{H}}\boldsymbol{J}_2\boldsymbol{Q}_M\}$. Eq. (19) can be expressed as

$$\mathrm{e}^{\mathrm{j}u_p^k/2}\left(\boldsymbol{K}_1-\mathrm{j}\boldsymbol{K}_2\right)\boldsymbol{d}_{px}^k=\mathrm{e}^{-\mathrm{j}u_p^k/2}\left(\boldsymbol{K}_1+\mathrm{j}\boldsymbol{K}_2\right)\boldsymbol{d}_{px}^k. \tag{20}$$

Then we can obtain the invariance relationship involving only real-valued quantities:

$$\tan\left(\frac{u_p^k}{2}\right)\boldsymbol{K}_1\boldsymbol{d}_{px}^k=\boldsymbol{K}_2\boldsymbol{d}_{px}^k. \tag{21}$$

If we define $\boldsymbol{K}_{u_1}=\boldsymbol{K}_1\otimes\boldsymbol{I}_N$ and $\boldsymbol{K}_{u_2}=\boldsymbol{K}_2\otimes\boldsymbol{I}_N$, the invariance for the real-valued manifold $\boldsymbol{d}_p^k$ satisfies

$$\tan\left(\frac{u_p^k}{2}\right)\boldsymbol{K}_{u_1}\boldsymbol{d}_p^k=\boldsymbol{K}_{u_2}\boldsymbol{d}_p^k. \tag{22}$$

Similarly, the real-valued manifold $\boldsymbol{d}_{py}^k$ satisfies $\tan(v_p^k/2)\boldsymbol{K}_3\boldsymbol{d}_{py}^k=\boldsymbol{K}_4\boldsymbol{d}_{py}^k$, where $\boldsymbol{K}_3$ and $\boldsymbol{K}_4$ are defined similar to $\boldsymbol{K}_1$ and $\boldsymbol{K}_2$ with M replaced by N, i.e., $\boldsymbol{K}_3=\mathrm{Re}\{\boldsymbol{Q}_{N-1}^{\mathrm{H}}\boldsymbol{J}_4\boldsymbol{Q}_N\}$ and $\boldsymbol{K}_4=\mathrm{Re}\{\boldsymbol{Q}_{N-1}^{\mathrm{H}}\boldsymbol{J}_4\boldsymbol{Q}_N\}$. Then we find that $\boldsymbol{d}_p^k$ satisfies

$$\tan\left(\frac{v_p^k}{2}\right)\boldsymbol{K}_{v_1}\boldsymbol{d}_p^k=\boldsymbol{K}_{v_2}\boldsymbol{d}_p^k, \tag{23}$$

where $\boldsymbol{K}_{v_1}=\boldsymbol{I}_M\otimes\boldsymbol{K}_3$ and $\boldsymbol{K}_{v_2}=\boldsymbol{I}_M\otimes\boldsymbol{K}_4$.

Consider the $MN\times P_k$ real-valued DOA matrix $\boldsymbol{D}_k=[\boldsymbol{d}_1^k,\boldsymbol{d}_2^k,\ldots,\boldsymbol{d}_{P_k}^k]$. Eqs. (22) and (23) indicate that $\boldsymbol{D}_k$ satisfies

$$\begin{cases}\boldsymbol{K}_{u_1}\boldsymbol{D}_k\boldsymbol{\Omega}_u^k=\boldsymbol{K}_{u_2}\boldsymbol{D}_k,\\ \boldsymbol{K}_{v_1}\boldsymbol{D}_k\boldsymbol{\Omega}_v^k=\boldsymbol{K}_{v_2}\boldsymbol{D}_k,\end{cases} \tag{24}$$

where $\boldsymbol{\Omega}_u^k=[\tan(u_1^k/2),\tan(u_2^k/2),\ldots,\tan(u_{P_k}^k/2)]$ and $\boldsymbol{\Omega}_v^k=[\tan(v_1^k/2),\tan(v_2^k/2),\ldots,\tan(v_{P_k}^k/2)]$.

If $\boldsymbol{E}_k$ denotes the $MN\times W$ complex-valued element space data matrix, as discussed in Zoltowski *et al.* (1996), the signal eigenvectors collected in $\boldsymbol{E}_\Lambda$ may be computed as the singular vectors associated with the P_k largest singular values of real-valued matrix $\boldsymbol{\Lambda}=[\mathrm{Re}\{\boldsymbol{B}_k\},\mathrm{Im}\{\boldsymbol{B}_k\}]$, where $\boldsymbol{B}_k=(\boldsymbol{Q}_M^{\mathrm{H}}\otimes\boldsymbol{Q}_N^{\mathrm{H}})\boldsymbol{E}_k$. As the number of snapshots $W\to\infty$, the subspace spanned by the columns of the $MN\times W$ real-valued matrix $\boldsymbol{E}_\Lambda$ becomes the same subspace spanned by the columns of the $MN\times W$ real-valued steering matrix $\boldsymbol{D}_k$. Therefore, we have $\boldsymbol{E}_\Lambda=\boldsymbol{D}_k\boldsymbol{T}$, in which $\boldsymbol{T}$ is an unknown $P_k\times P_k$ full rank real-valued matrix. Substituting $\boldsymbol{D}_k=\boldsymbol{E}_\Lambda\boldsymbol{T}^{-1}$ into Eq. (24) yields

$$\begin{cases}\boldsymbol{K}_{u_1}\boldsymbol{E}_\Lambda\boldsymbol{\Psi}_u^k=\boldsymbol{K}_{u_2}\boldsymbol{E}_\Lambda,\ \ \boldsymbol{\Psi}_u^k=\boldsymbol{T}^{-1}\boldsymbol{\Omega}_u^k\boldsymbol{T},\\ \boldsymbol{K}_{v_1}\boldsymbol{E}_\Lambda\boldsymbol{\Psi}_v^k=\boldsymbol{K}_{v_2}\boldsymbol{E}_\Lambda,\ \ \boldsymbol{\Psi}_v^k=\boldsymbol{T}^{-1}\boldsymbol{\Omega}_v^k\boldsymbol{T}.\end{cases} \tag{25}$$

According to Eq. (25), $\boldsymbol{\Psi}_u^k$ and $\boldsymbol{\Psi}_v^k$ can be solved by the LS or total LS (TLS) algorithm. Automatic pairing of spatial frequency estimates u_p^k and v_p^k is facilitated by the fact that all of the quantities in Eq. (25) are real values. Thus, $\boldsymbol{\Psi}_u^k+\mathrm{j}\boldsymbol{\Psi}_v^k$ may be spectrally decomposed as

$$\boldsymbol{\Psi}_u^k+\mathrm{j}\boldsymbol{\Psi}_v^k=\boldsymbol{T}^{-1}\{\boldsymbol{\Omega}_u^k+\mathrm{j}\boldsymbol{\Omega}_v^k\}\boldsymbol{T}. \tag{26}$$

Accordingly, u_p^k and v_p^k $(p=1,2,\ldots,P_k)$ can be estimated based on the eigenvalues of Eq. (26) (denoted by $\hat{\eta}_p^k$):

$$\begin{cases}\hat{u}_p^k=2\arctan\left\{\mathrm{Re}\left(\hat{\eta}_p^k\right)\right\},\\ \hat{v}_p^k=2\arctan\left\{\mathrm{Im}\left(\hat{\eta}_p^k\right)\right\}.\end{cases} \tag{27}$$

From the defination of the spatial frequency, we can obtain the paired 2D angle automatically:

$$\begin{cases}\hat{\varphi}_p^k=\arctan\left(\dfrac{\hat{v}_p^k}{\hat{u}_p^k}\right),\\ \hat{\theta}_p^k=\arcsin\sqrt{\left(\hat{u}_p^k\dfrac{\lambda}{2\pi d}\right)^2+\left(\hat{v}_p^k\dfrac{\lambda}{2\pi d}\right)^2}.\end{cases} \tag{28}$$

As we can see, the proposed algorithm can obtain the closed form of DOA as Eq. (28) and the automatic pairing of azimuth and elevation angles using the real and imaginary parts of the eigenvalues in Eq. (27). The algorithm does not need the spectrum peak search or pairing processes, so it reduces the computational burden.

3.3 Directional channel estimation

The estimated combined channel impulse responses for the kth user can be expressed based on

Eq. (6), which is extended as

$$\hat{\boldsymbol{G}}_k = \boldsymbol{H}_k \boldsymbol{A}_k^{\mathrm{T}} + \boldsymbol{U}_k, \tag{29}$$

where $\boldsymbol{U}_k$ is the estimation error. According to the estimated combined channel impulse responses $\hat{\boldsymbol{G}}_k$ and the estimated steering matrix $\hat{\boldsymbol{A}}_k$, the directional channel impulse responses can be estimated as

$$\hat{\boldsymbol{H}}_k = \hat{\boldsymbol{G}}_k \left(\hat{\boldsymbol{A}}_k^{\mathrm{T}}\right)^{\dagger}. \tag{30}$$

4 Data detection

In this section, a novel technique for data detection of all the users in the massive MIMO systems is presented. This technique takes into account the DOAs of signals and the associated directional channel impulse responses.

Assume that K users are simultaneously active transmitting complex data symbols s_d^k ($d = 1, 2, \cdots, D$, $k = 1, 2, \cdots, K$). The data symbols from user k are held in vector $\boldsymbol{s}^k = [s_1^k, s_2^k, ..., s_D^k]^{\mathrm{T}} \in \mathbb{C}^{D\times 1}$, and the data symbols from all K users can be combined to the vector

$$\boldsymbol{s} = [(\boldsymbol{s}^1)^{\mathrm{T}}, (\boldsymbol{s}^2)^{\mathrm{T}}, \ldots, (\boldsymbol{s}^K)^{\mathrm{T}}]^{\mathrm{T}} \in \mathbb{C}^{KD\times 1}. \tag{31}$$

With the directional channel impulse response estimates (Eq. (30)), we form matrices $\boldsymbol{H}_{Dp}^k \in \mathbb{C}^{(D+W-1)\times D}$ as

$$\boldsymbol{H}_{Dp}^k = \begin{bmatrix} h_{p1}^k & & 0 \\ h_{p2}^k & \ddots & \vdots \\ \vdots & \ddots & h_{p1}^k \\ h_{pW}^k & & h_{p2}^k \\ \vdots & \ddots & \vdots \\ 0 & & h_{pW}^k \end{bmatrix}. \tag{32}$$

Based on the $P_k(D+W-1)\times D$ matrix $\boldsymbol{H}_D^k = [(\boldsymbol{H}_{D1}^k)^{\mathrm{T}}, (\boldsymbol{H}_{D2}^k)^{\mathrm{T}}, \ldots, (\boldsymbol{H}_{DP_k}^k)^{\mathrm{T}}]^{\mathrm{T}}$, which contains the directional channel impulse responses corresponding to the kth user, we define the $(\sum_{k=1}^K P_k)(D+W-1)\times KD$ block diagonal matrix

$$\boldsymbol{H}_D = \mathrm{blockdiag}[\boldsymbol{H}_D^1, \boldsymbol{H}_D^2, \ldots, \boldsymbol{H}_D^K]. \tag{33}$$

Furthermore, the array steering matrix $\boldsymbol{A}_k$ for the kth user can be combined to matrix

$$\boldsymbol{A} = [\boldsymbol{A}_1, \boldsymbol{A}_2, \ldots, \boldsymbol{A}_K] \in \mathbb{C}^{MN\times(\sum_{k=1}^K P_k)}, \tag{34}$$

and then the following definition is introduced:

$$\begin{aligned} \boldsymbol{A}_D &= \boldsymbol{A} \otimes \boldsymbol{I}_{D+W-1} \\ &\in \mathbb{C}^{MN(D+W-1)\times(\sum_{k=1}^K P_k)(D+W-1)}. \end{aligned} \tag{35}$$

The signal received at the ith antenna $\underline{\boldsymbol{y}}_i \in \mathbb{C}^{(D+W-1)\times 1}$ ($i = 1, 2, \ldots, MN$) depends exclusively on the transmitted data symbols but not on the training sequences. These MN vectors can be arranged in the $(D+W-1)\times MN$ matrix

$$\underline{\boldsymbol{Y}} = [\underline{\boldsymbol{y}}_1, \underline{\boldsymbol{y}}_2, \ldots, \underline{\boldsymbol{y}}_{MN}]. \tag{36}$$

Then, the combined signal received at all MN antennas can be expressed as

$$\underline{\boldsymbol{y}} = \mathrm{vec}\{\underline{\boldsymbol{Y}}\}. \tag{37}$$

Then, according to Eqs. (31), (33), and (35), the combined signal received can be expressed as

$$\underline{\boldsymbol{y}} = \boldsymbol{A}_D \boldsymbol{H}_D \boldsymbol{S} + \boldsymbol{f}, \tag{38}$$

where $\boldsymbol{f}$ is the combined noise vector at all MN array elements. Then, the data detected is

$$\hat{\boldsymbol{s}} = (\boldsymbol{A}_D \boldsymbol{H}_D)^{\dagger} \underline{\boldsymbol{y}}. \tag{39}$$

As in the massive MIMO systems, matrix $\boldsymbol{A}_D\boldsymbol{H}_D \in \mathbb{C}^{MN(D+W-1)\times KD}$ is very large and its pseudoinverse is a huge challenge. Thus, we will discuss $((\boldsymbol{A}_D\boldsymbol{H}_D)^{\mathrm{H}}\boldsymbol{A}_D\boldsymbol{H}_D)^{-1}$ next and the following theorem is given first:

Theorem 1 For a URA with azimuth and elevation angles of arrival drawn independently from a continuous distribution, the steering vectors are orthogonal as the number of antenna elements, MN, tends to infinity, i.e.,

$$\frac{1}{MN}\boldsymbol{A}^{\mathrm{H}}\boldsymbol{A} = \boldsymbol{I}_{\sum_{k=1}^K P_k}. \tag{40}$$

Proof Let $\boldsymbol{a}_p^k$ and $\boldsymbol{a}_q^l$ be the different columns in $\boldsymbol{A}$ ($k = 1, 2, \ldots, K$, $p = 1, 2, \ldots, P_k$, $k \neq l$ or $p \neq q$). The steering vectors of the URA can be decomposed into a Kronecker product of two ULA responses as Eq. (14), and then we can express $\left|(\boldsymbol{a}_p^k)^{\mathrm{H}}(\boldsymbol{a}_q^l)\right|$ as

$$\begin{aligned} \left|(\boldsymbol{a}_p^k)^{\mathrm{H}}(\boldsymbol{a}_q^l)\right| &= \left|\left(\boldsymbol{a}_{xp}^k \otimes \boldsymbol{a}_{yp}^k\right)^{\mathrm{H}}\left(\boldsymbol{a}_{xq}^l \otimes \boldsymbol{a}_{yq}^l\right)\right| \\ &= \left|\left((\boldsymbol{a}_{xp}^k)^{\mathrm{H}}\boldsymbol{a}_{xq}^l\right) \otimes \left((\boldsymbol{a}_{yp}^k)^{\mathrm{H}}\boldsymbol{a}_{yq}^l\right)\right| \\ &= \left|\sum_{m=1}^{M} \mathrm{e}^{\mathrm{j}(m-(M+1)/2)(u_q^l - u_p^k)}\right. \\ &\quad \left.\cdot \sum_{n=1}^{N} \mathrm{e}^{\mathrm{j}(n-(N+1)/2)(v_q^l - v_p^k)}\right|. \end{aligned} \tag{41}$$

φ_p^k and φ_q^l as well as θ_p^k and θ_q^l are chosen independently from a continuous distribution; consequently, $u_q^l - u_p^k \neq 0$ as well as $v_q^l - v_p^k \neq 0$ with probability one. Therefore, the two geometric series in Eq. (41) have the ratios $\mathrm{e}^{\mathrm{j}(u_q^l - u_p^k)} \neq 1$ and $\mathrm{e}^{\mathrm{j}(v_q^l - v_p^k)} \neq 1$. Thus,

$$\begin{aligned}\left|(\boldsymbol{a}_p^k)^{\mathrm{H}}(\boldsymbol{a}_q^l)\right| &= \frac{|\mathrm{e}^{\mathrm{j}(-(M-1)/2)(u_q^l-u_p^k)}(1-\mathrm{e}^{\mathrm{j}(u_q^l-u_p^k)M})|}{|1-\mathrm{e}^{\mathrm{j}(u_q^l-u_p^k)}|} \\ &\quad \cdot \frac{|\mathrm{e}^{\mathrm{j}(-(N-1)/2)(v_q^l-v_p^k)}(1-\mathrm{e}^{\mathrm{j}(v_q^l-v_p^k)N})|}{|1-\mathrm{e}^{\mathrm{j}(v_q^l-v_p^k)}|} \\ &\leq \frac{4}{|1-\mathrm{e}^{\mathrm{j}(u_q^l-u_p^k)}||1-\mathrm{e}^{\mathrm{j}(v_q^l-v_p^k)}|}.\end{aligned} \tag{42}$$

Let $\boldsymbol{A}^{-p^k}$ represent the steering matrix $\boldsymbol{A}$ with the steering vector for the pth path of the kth user removed. Based on Eq. (42), the magnitude of the projection of the vector $\boldsymbol{a}_p^k$ onto span$\{C(\boldsymbol{A})\}$ is upper bounded by

$$\begin{aligned}&\lim_{MN\to\infty}\frac{1}{MN}\left\|(\boldsymbol{a}_p^k)^{\mathrm{H}}\boldsymbol{A}^{-p^k}\right\| \\ &\leq \lim_{MN\to\infty}\frac{1}{MN}\sum_{\substack{l\neq k \text{ or} \\ q\neq p}}\left|(\boldsymbol{a}_p^k)^{\mathrm{H}}\boldsymbol{a}_q^l\right| \\ &= 0.\end{aligned}$$

This proves Eq. (40).

According to Theorem 1, we can obtain

$$\begin{aligned}\boldsymbol{A}_D^{\mathrm{H}}\boldsymbol{A}_D &= (\boldsymbol{A}\otimes\boldsymbol{I}_{D+W-1})^{\mathrm{H}}(\boldsymbol{A}\otimes\boldsymbol{I}_{D+W-1}) \\ &= (\boldsymbol{A}^{\mathrm{H}}\boldsymbol{A})\otimes(\boldsymbol{I}_{D+W-1}^{\mathrm{H}}\boldsymbol{I}_{D+W-1}) \\ &\approx MN\boldsymbol{I}_{\sum_{k=1}^K P_k}\otimes\boldsymbol{I}_{D+W-1} \\ &= MN\boldsymbol{I}_{(\sum_{k=1}^K P_k)\times(D+W-1)}.\end{aligned} \tag{43}$$

After this, we can rewrite $((\boldsymbol{A}_D\boldsymbol{H}_D)^{\mathrm{H}}(\boldsymbol{A}_D\boldsymbol{H}_D))^{-1}$ as

$$\begin{aligned}&((\boldsymbol{A}_D\boldsymbol{H}_D)^{\mathrm{H}}\boldsymbol{A}_D\boldsymbol{H}_D))^{-1} \\ &= (\boldsymbol{H}_D^{\mathrm{H}}\boldsymbol{A}_D^{\mathrm{H}}\boldsymbol{A}_D\boldsymbol{H}_D)^{-1} \\ &\approx (\boldsymbol{H}_D^{\mathrm{H}}MN\boldsymbol{I}_{(\sum_{k=1}^K P_k)\times(D+W-1)}\boldsymbol{H}_D)^{-1} \\ &= \frac{(\mathrm{blockdiag}[\boldsymbol{H}_{D1}^{\mathrm{H}}\boldsymbol{H}_{D1},\ldots,\boldsymbol{H}_{DK}^{\mathrm{H}}\boldsymbol{H}_{DK}])^{-1}}{MN} \\ &= \frac{\mathrm{blockdiag}[(\boldsymbol{H}_{D1}^{\mathrm{H}}\boldsymbol{H}_{D1})^{-1},...,(\boldsymbol{H}_{DK}^{\mathrm{H}}\boldsymbol{H}_{DK})^{-1}]}{MN} \\ &\triangleq \boldsymbol{\Gamma}.\end{aligned} \tag{44}$$

Then, an inverse of the $KD\times KD$ matrix is transformed to K inverses of a $D\times D$ matrix. The complexity of a $D\times D$ matrix inverse is $O(D^3)$. Thus, the complexity of the data detection is reduced from $O(K^3D^3)$ to $O(D^3)$. Then, the data detected can be obtained approximately with a lower computational complexity

$$\hat{\boldsymbol{s}} \approx \boldsymbol{\Gamma}(\boldsymbol{A}_D\boldsymbol{H}_D)^{\mathrm{H}}\underline{\boldsymbol{y}}. \tag{45}$$

The proposed estimation algorithm is summarized in Algorithm 1.

Algorithm 1 Joint DOA and channel estimation with data detection

1: Estimate the combined channel impulse responses $\hat{\boldsymbol{G}}$ by the training sequence $\boldsymbol{X}$ according to Eq. (8)
2: **for** $k=1$ to K **do**
3: Extract $\hat{\boldsymbol{G}}_k$ from $\hat{\boldsymbol{G}}$ using Eq. (10)
4: Compute the signal subspace $\boldsymbol{E}_\Lambda$ via the P_k largest left singular vectors of $[\mathrm{Re}\{\boldsymbol{B}_k\},\mathrm{Im}\{\boldsymbol{B}_k\}]$, where $\boldsymbol{B}_k=(\boldsymbol{Q}_M^H\otimes\boldsymbol{Q}_N^H)\boldsymbol{E}_k$ and $\boldsymbol{E}_k=\hat{\boldsymbol{G}}_k^{\mathrm{T}}$
5: Compute $\boldsymbol{\Psi}_u$ and $\boldsymbol{\Psi}_v$ as the solution to Eq. (25)
6: Compute $\hat{\eta}_p^k$ $(p=1,2,\ldots,P_k)$ as the eigenvalues of the $P_k\times P_k$ matrix $\boldsymbol{\Psi}_u+\mathrm{j}\boldsymbol{\Psi}_v$
7: Compute $\hat{\varphi}_p^k$ and $\hat{\theta}_p^k$ using Eq. (28)
8: Calculate the directional channel impulse responses $\hat{\boldsymbol{H}}_k$ according to Eq. (30)
9: **end for**
10: Detect the data using the estimated directional channel impulse and steering matrix according to Eq. (45)

5 Simulation results

In this section, we investigate the performance of the proposed estimator through 10 000 Monte-Carlo simulations based on a URA with $d=\lambda/2$. The source scenario consists of $K=2$ equipowered, uncorrelated sources with $P_k=2$ $(k=1,2)$ paths located at angles $\phi_1^1=30°,\phi_2^1=60°,\theta_1^1=10°,\theta_2^1=35°$ for user 1 and $\phi_1^2=45°,\phi_2^2=50°,\theta_1^2=20°,\theta_2^2=55°$ for user 2. The noise variance is $\sigma_{\mathrm{n}}^2=1$. The transmitted signals, $s_k(t)$ $(k=1,2)$, are quadrature phase shift keying (QPSK) modulated. The lengths of the training sequence and data are $L=200$ and $D=500$, respectively.

The normalized mean square errors (NMSEs) of the estimated channel impulse responses versus SNR for different numbers of BS antennas are depicted in Fig. 2. The NMSEs of the combined (Eq. (18)) and directional (Eq. (29)) channel impulse response estimates are shown. It can be seen that all the NMSEs decrease rapidly as the SNR increases. It is obvious that the NMSEs of the combined channel

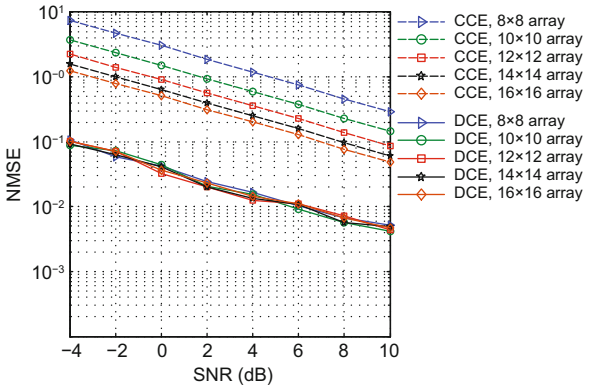

Fig. 2 Normalized mean square errors (NMSEs) of channel estimation versus SNR (CCE: combined channel estimation using Eq. (8); DCE: directional channel estimation using Eq. (29))

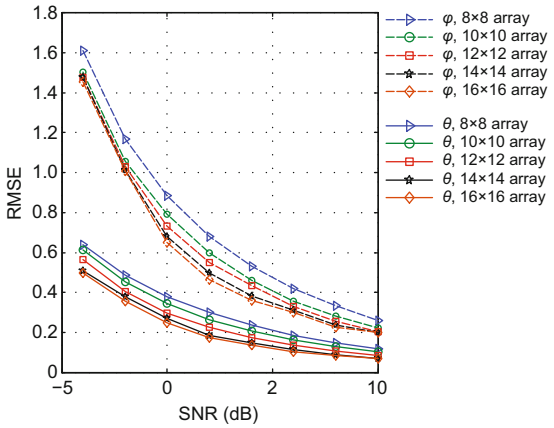

Fig. 3 The root-mean-square errors (RMSEs) of azimuth angle φ and elevation angle θ estimates versus SNR

impulse response estimations decrease as the number of antennas becomes larger, while the NMSEs of the directional channel impulse response estimations are insensitive to the number of antennas.

The root-mean-square errors (RMSEs) of the estimated DOAs versus SNR under different numbers of antennas are shown in Fig. 3. It can be observed that the RMSEs of the azimuth angle φ and elevation angle θ for different numbers of antennas decrease rapidly when the SNR increases. The RMSEs also decrease as the number of antennas becomes large. However, the RMSEs do not change very much when the total number of antennas is 16×16 compared to that of 14×14. Thus, the effect of increasing the number of BS antennas is similar to that of increasing SNR. In other words, in massive MIMO systems, the transmitted power can be significantly reduced for an appropriately large number of BS antennas.

Fig. 4 gives the simulation of the bit-error rate (BER) performance versus the SNR. The performance of a larger number of antennas (such as 16×16) is better because the DOA estimates become more accurate for the larger number of antennas. The small gaps in BERs between the data detected using Eqs. (45) and (39) verify that the performance of the proposed low-complexity data detection algorithm is similar to that of the original algorithm. Thus, we can further prove Theorem 1 by this simulation. Fig. 5 compares the computational complexities versus the data length. It can be concluded from Figs. 4 and 5 that the proposed data detection algorithm is easier to compute than the conventional algorithm with a similar performance in BER.

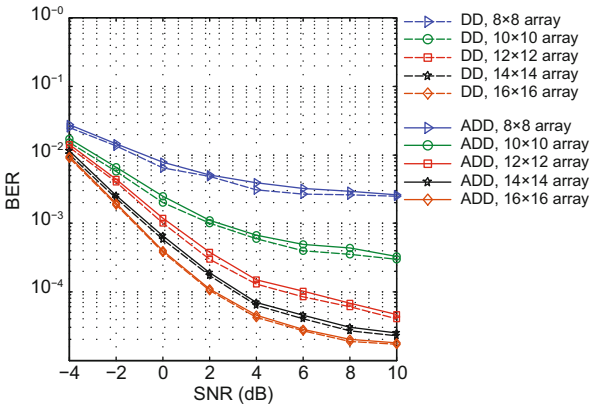

Fig. 4 Bit-error rates of data detection versus SNR (DD: data detection using Eq. (38); ADD: low-complexity approximate data detection using Eq. (44))

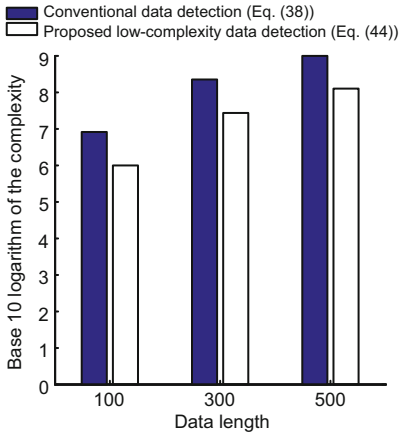

Fig. 5 Computational complexities of data detection algorithms versus the data length

6 Conclusions

In this paper, a novel joint DOA and channel estimation with data detection is proposed for URAs in a massive MIMO system. The conventional channel impulse responses for the links between the transmitters and antenna elements are first estimated through known training sequences, and then 2D DOAs are estimated based on a 2D unitary ESPRIT algorithm without searching and pairing processes. As the information about the DOAs can be exploited to estimate the channels associated with the different DOAs, the enhanced channel impulse responses estimated are obtained. Moreover, a low-complexity data detection technique is presented. Simulation results show that the proposed method can jointly estimate DOA and channel impulse responses and detect data effectively with a good performance.

References

Alibi, D., Javed, U., Wen, F., *et al.*, 2016. 2D DOA estimation method based on channel state information for uniform circular array. 4th Int. Conf. on Ubiquitous Positioning, Indoor Navigation and Location Based Services, p.68-72. http://dx.doi.org/10.1109/UPINLBS.2016.7809952

Barabell, A., 1983. Improving the resolution performance of eigenstructure-based direction finding algorithm. IEEE Int. Conf. on Acoustics, Speech, and Signal Processing, p.336-339. http://dx.doi.org/10.1109/ICASSP.1983.1172124

Blanz, J.J., Papathanassiou, A., Haardt, M., *et al.*, 2000. Smart antennas for combined DOA and joint channel estimation in time-slotted CDMA mobile radio systems with joint detection. *IEEE Trans. Veh. Technol.*, **49**(2):293-306. http://dx.doi.org/10.1109/25.832962

Capon, J., 1983. Maximum-likelihood spectral estimation. *In*: Haykin, S. (Ed.), Nonlinear Methods of Spectral Analysis. Springer Berlin Heidelberg, p.155-179. http://dx.doi.org/10.1007/3-540-12386-5_12

D'Amico, A.A., Morelli, M., 2009. Joint channel and DOA estimation for multicarrier CDMA uplink transmissions. *IEEE Trans. Veh. Technol.*, **58**(1):116-125. https://dx.doi.org/10.1109/TVT.2008.921624

D'Amico, A.A., Mengali, U., Morelli, M., 2004. DOA and channel parameter estimation for wideband CDMA systems. *IEEE Trans. Wirel. Commun.*, **3**(6):1942-1947. http://dx.doi.org/10.1109/TWC.2004.837446

Haardt, M., Nossek, J.A., 1995. Unitary ESPRIT: how to obtain increased estimation accuracy with a reduced computational burden. *IEEE Trans. Signal Process.*, **43**(5):1232-1242. http://dx.doi.org/10.1109/78.382406

Hu, A., Lv, T., Gao, H., *et al.*, 2014. An ESPRIT-based approach for 2-D localization of incoherently distributed sources in massive MIMO systems. *IEEE J. Sel. Topics Signal Process.*, **8**(5):996-1011. http://dx.doi.org/10.1109/JSTSP.2014.2313409

Lan, X., Li, Y., Wang, E., 2016. A RARE algorithm for 2D DOA estimation based on nested array in massive MIMO system. *IEEE Access*, **4**:3806-3814. http://dx.doi.org/10.1109/ACCESS.2016.2583458

Larsson, E.G., Edfors, O., Tufvesson, F., *et al.*, 2014. Massive MIMO for next generation wireless systems. *IEEE Commun. Mag.*, **52**(2):186-195. http://dx.doi.org/10.1109/MCOM.2014.6736761

Liu, L., Li, Y., Zhang, J., 2014. DoA estimation and achievable rate analysis for 3D millimeter wave massive MIMO systems. IEEE 15th Int. Workshop on Signal Processing Advances in Wireless Communications, p.6-10. http://dx.doi.org/10.1109/SPAWC.2014.6941306

Marzetta, T.L., 2010. Noncooperative cellular wireless with unlimited numbers of base station antennas. *IEEE Trans. Wirel. Commun.*, **9**(11):3590-3600. http://dx.doi.org/10.1109/TWC.2010.092810.091092

Roy, R., Kailath, T., 1989. ESPRIT-estimation of signal parameters via rotational invariance techniques. *IEEE Trans. Acoust. Speech Signal Process.*, **37**(7):984-995. http://dx.doi.org/10.1109/29.32276

Rusek, F., Persson, D., Lau, B.K., *et al.*, 2013. Scaling up MIMO: opportunities and challenges with very large arrays. *IEEE Signal Process. Mag.*, **30**(1):40-60. http://dx.doi.org/10.1109/MSP.2011.2178495

Schmidt, R., 1986. Multiple emitter location and signal parameter estimation. *IEEE Trans. Antennas Propag.*, **34**(3):276-280. http://dx.doi.org/10.1109/TAP.1986.1143830

Wang, A., Liu, L., Zhang, J., 2012. Low complexity direction of arrival (DoA) estimation for 2D massive MIMO systems. IEEE GLOBECOM Workshops, p.703-707. http://dx.doi.org/10.1109/GLOCOMW.2012.6477660

Wang, T., Ai, B., He, R., *et al.*, 2015. Two-dimension direction-of-arrival estimation for massive MIMO systems. *IEEE Access*, **3**:2122-2128. http://dx.doi.org/10.1109/ACCESS.2015.2496944

Yang, K., Wu, J., Li, W., 2014. A low-complexity direction-of-arrival estimation algorithm for full-dimension massive MIMO systems. IEEE Int. Conf. on Communication Systems, p.472-476. http://dx.doi.org/10.1109/ICCS.2014.7024848

Zhang, R., Wang, S., Zhong, Z., *et al.*, 2015. Multipath DOA estimation by rotational invariance on array channel impulse response. *IEEE Antennas Wirel. Propag. Lett.*, **15**:964-967. http://dx.doi.org/10.1109/LAWP.2015.2486624

Zhu, Y., Liu, L., Wang, A., *et al.*, 2013. DoA estimation and capacity analysis for 2D active massive MIMO systems. IEEE Int. Conf. on Communications, p.4630-4634. http://dx.doi.org/10.1109/ICC.2013.6655301

Zoltowski, M.D., Haardt, M., Mathews, C.P., 1996. Closed-form 2-D angle estimation with rectangular arrays in element space or beamspace via unitary ESPRIT. *IEEE Trans. Signal Process.*, **44**(2):316-328. http://dx.doi.org/10.1109/78.485927